ARMY RESEARCH LABORATORY

Modeling Ceramic Defeat Mechanisms and Variations in Ballistic Data

by Nevin L. Rupert
and Fred I. Grace

ARL-TR-1670

May 1998

Army Research Laboratory
Aberdeen Proving Ground, MD 21005-5066

ARL-TR-1670 **May 1998**

Modeling Ceramic Defeat Mechanisms and Variations in Ballistic Data

Nevin L. Rupert, Fred I. Grace
Weapons and Materials Research Directorate, ARL

Abstract

Bi-element or layered targets have been used to obtain depth-of-penetration (DOP) data so that performance of ceramic materials under ballistic impact can be evaluated. While the data have been particularly useful for ranking ceramics as possible armor candidates, interpretation of the data has been difficult and little insight into the dynamics and mechanisms of the penetration process has been obtained from such data. Prior analytical work into the penetration mechanics of ceramics by the authors included two important factors (i.e., a dynamic target interaction resulting from pressure wave reflection at the interface between target elements and a time-dependent damage mechanism describing the response of the ceramic material). In the present work, a "size" effect, known to be associated with ceramic behavior, and the introduction of a third process zone have been included in the analysis to address a portion of the variations (scatter) in the DOP test data. The analysis now includes results of the weakest-link theory in terms of the Weibull distribution and measured parameters for Al_2O_3. Calculated results are compared with the original data and prior analysis to provide relationships between all three mechanisms and indicate the influence of the size effect on the data.

Table of Contents

Page

INTENTIONALLY LEFT BLANK

List of Figures

List of Tables

INTENTIONALLY LEFT BLANK

1. Introduction

The use of semi-infinite, bi-element targets in depth-of-penetration (DOP) tests initially arose from the need to determine the performance potential of ceramic materials under ballistic impact. However, since ceramics exhibit complex damage responses, interpretation of DOP results for ceramic/metal target combinations has been difficult. The previous work by Rupert and Grace (1993) and Grace and Rupert (1993) had identified a dynamic effect referred to as a "density" effect mechanism (Rupert and Grace 1994) for both metallic and ceramic appliques. This effect is the result of a pressure wave reflecting from a higher density second element and its associated material particle velocity, which moves back toward the penetrator. This motion enhances the penetration rate in the first element with corresponding reduction in penetrator erosion rate. Thus, a greater uneroded rod length reaches the bi-element interface, which produces greater penetration into the second element. When a second element has the lower density, an opposite condition exists. The relief wave moves material away from the penetrator, lowers penetration rates, increases rod erosion rates, and lowers uneroded rod length. In that case, penetration into the second element may be expected to be somewhat lower. This work demonstrates that significant target interactions are present in addition to specific time-dependent damage mechanisms inherent in the ceramic response. Through the analytical model (Grace and Rupert 1993; Grace 1993), the density effect and time-dependent mechanisms were separated so that the role of each factor could be evaluated. Even so, there appears to be some scatter in test results that could not be addressed by the inclusion of the previously mentioned dynamic interactions. Thus, the current work extends the model by introducing the Weibull (1939; 1951) distribution and a third process zone as initial steps in interpreting the upper and lower performance limits bounding the scatter in ceramic data.

An experimental process used to evaluate a ceramic is the DOP test as described by Woolsey, Mariano, and Kokidko (1989). Such tests make use of a well-characterized penetrator that is fired into a ceramic/ metal layered target (i.e., bi-element target), where the second element (i.e., metal) is sufficiently thick to be considered semi-infinite. The penetration depth (or DOP) is measured in the metal that is typically rolled homogeneous armor (RHA). DOP results can be compared with penetration into a single-element, semi-infinite metal target. Quite often, DOP results show a considerable degree of inherit scatter, even where the dimensional tolerances for the targets and impact conditions are well controlled. A factor that can influence penetration in ceramics is strength. It is well known that the strength of ceramic materials, unlike metals, is limited by the size of inherent flaws through a Griffith's-type relationship (Griffith 1924). These flaws can vary considerably in size. (In addition, failure in a stressed ceramic component follows the weakest link theory, which states that failure is determined by the lowest stress at the most critical flaw that initiates crack growth.) This phenomena yields a size dependence of stress referred to as "size" effect (McClintock and Argon 1966). As a result, strengths tend to vary with ceramic thickness and require statistical description of this strength variation (Jadaan et al. 1991). Since strength is an important consideration in penetration, the variations in this parameter for ceramics need to be considered in analyses of ballistic tests. The current work describes how the Weibull distribution has been introduced into the previous penetration model (Rupert and Grace 1996) to describe the ceramics intrinsic variation in performance and compares the new results with experimental DOP data for Al_2O_3.

2. Statement of the Problem

Previous results for Al_2O_3/RHA targets impacted by a depleted uranium (DU) alloy penetrator are shown in Figure 1 to include the data (circled points) reported by Woolsey, Mariano, and Kokidko (1989) and the analysis of Grace and Rupert (1993). Woolsey identified four regions (as shown in Figure 2) based on changes in the graphical appearance of the data when DOP results vs. ceramic applique thickness are plotted. Grace and Rupert (1993) offered physical explanations as to what would cause the DOP data to change within these four regions. In region I, a dynamic target interaction effect is present and is the dominant defeat mechanism for thinner ceramic sections. The significant performance gains in region II were explained in terms of the ceramic acting initially as a nearly intact material. The slope of region II is determined by the introduction of the time-dependent damage mechanisms resulting in a mixed solid/granular flow and the rate of transition from mixed solid/granular flow to pure granular flow. Region III was defined as a region where pure

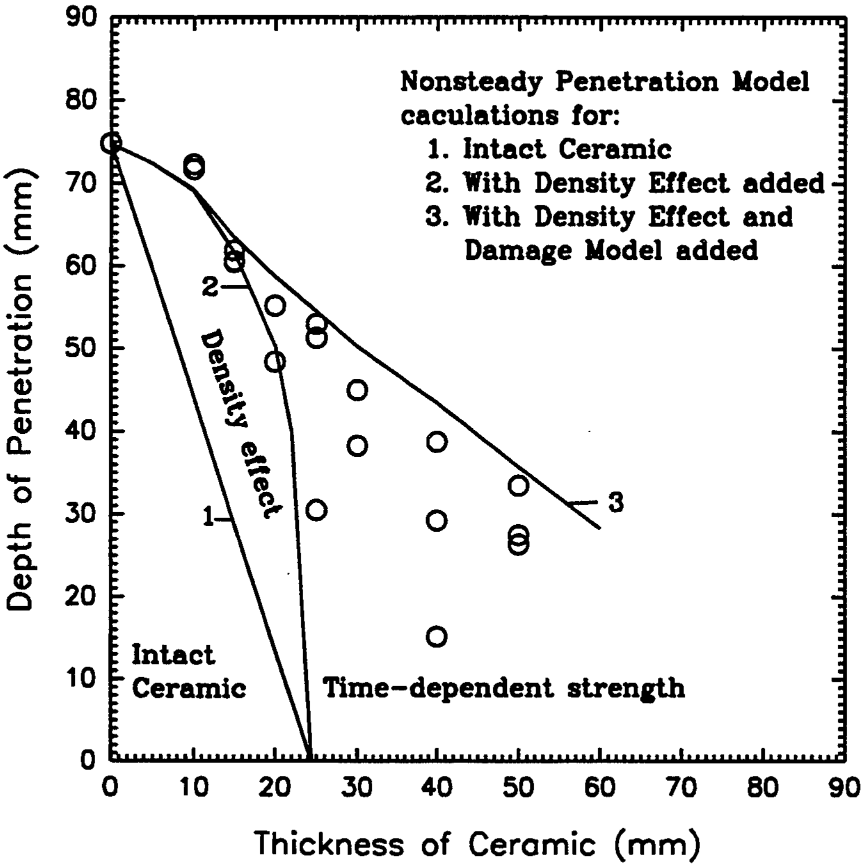

Figure 1. Model Results for Al_2O_3/RHA Against the 65-g L/D 10 Depleted Uranium Laboratory Penetrator at 1,500 m/s (Grace and Rupert 1993).

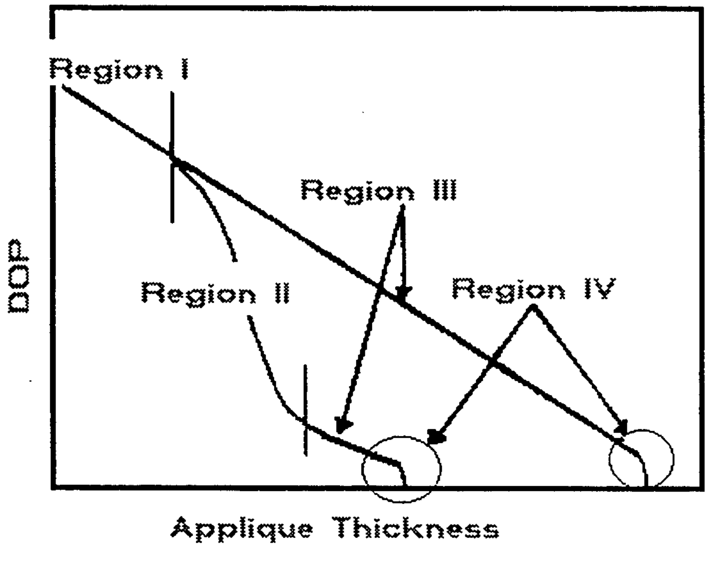

Figure 2. Generalized Performance Map for Ceramic DOP Tests Identifying the Four Regions of Performance.

granular flow becomes the dominant damage mechanism. Region IV is the termination phase where the unconsumed portion of rod traveling at low velocity abruptly decelerates and stops.

In previous work, Rupert and Grace (1993) experimentally investigated an all-metal, bi-element target of Ti alloy/RHA. These metallic targets exhibited similar behavior as that found in ceramic/metal targets associated with region I (see Figure 3). Further, this effect persisted throughout thickness increases mimicking regions II and III. Since the Ti alloy properties are essentially independent of thickness over the range of applique thickness tested in contrast to the time-dependent strength that can occur in ceramics, the effect in the ceramic could not considered to be an outgrowth of strength degradation. Further, reversing the order of materials in the metal layers produced a slight reduction in the penetration rate and increased rod erosion rate. For these particular metals, reversing the material order reversed the material densities significantly, but did not change the strengths appreciably (see Figure 4). Thus, the observed effect was considered to be associated with the dynamics of target interaction involving mismatch of densities at the metal/metal interface.

In modeling bi-element ceramic/metal penetration, Grace and Rupert (1993) utilized both (1) the density effect, as described previously, and (2) a time-dependent damage concept for the ceramic (Curran et al. 1993; Cortés et al. 1992). The introduction of damage functions, together with the density effect, provided a penetration algorithm that produced the DOP performance envelopes for the ceramic as shown in Figure 1 (solid lines). The details of the calculations provided physical explanations for the regions as described in section 3.

Figure 1 also shows considerable scatter in the DOP test data that was not explained by the previous penetration model dynamic analysis. Thus, the problem of interest here is to address the variations in the data by taking into account, as a first step, the "size" effect described earlier together with the associated Weibull distribution and the introduction of a third process zone. The influence of these additional factors on the DOP performance envelope for Al_2O_3, as previously illustrated in Figure 1, is analyzed.

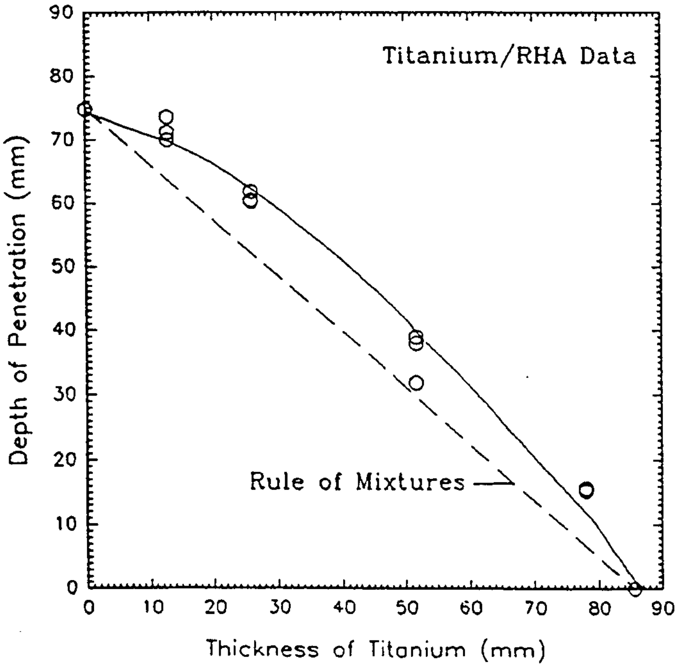

Figure 3. Velocity Corrected Titanium/RHA DOP Data Against the 65-g L/D 10 Tungsten Laboratory Penetrator at 1,500 m/s (Rupert and Grace 1995).

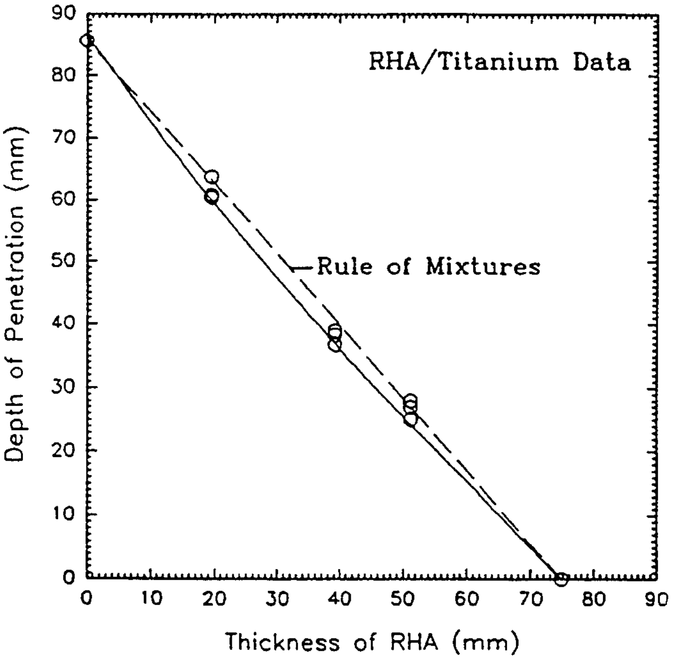

Figure 4. Velocity Corrected RHA/Titanium DOP Data Against the 65-g L/D 10 Tungsten Laboratory Penetrator at 1,500 m/s (Rupert and Grace 1995).

3. Review of the Penetration Analysis

3.1 The Penetration Integral and Velocity Solutions. The analytical approach to the DOP problem is an application of the nonsteady penetration development of Grace (1993). The theory deals with the penetration of long-rod penetrators into monolithic, semi-infinite targets. The application to DOP bi-element-type targets was provided by Grace and Rupert (1993). The geometry of the bi-element target is shown in Figure 5. Impact conditions are rod impact velocity v_s, initial rod length ℓ_o, and first-element thickness a_o. The backup target, or second element, is semi-infinite metal. To begin penetration of the second layer, the velocity v_1 and rod length ℓ_1 that exist at the interface between targets must be determined. These quantities depend, of course, upon rod length and velocity losses that occur during penetration through the first layer. For the bi-element target, it is assumed that the total penetration P_T in the overall target is the sum of that through each element. This gives

$$P_T = -\int_{\ell_o}^{\ell_1} \left(\frac{u}{v-u}\right)_1 dl - \int_{\ell_1}^{\ell_2} \left(\frac{u}{v-u}\right)_2 dl, \tag{1}$$

where u is the penetration rate, v is the penetrator velocity, and $(u/(v-u))_1$ and $(u/(v-u))_2$ are respective velocities for the two elements. When the penetrator can overmatch the first element, the first integral on the right-hand side of equation (1) is equal to the first element thickness, which is designated a_o. Therefore, the DOP or residual penetration P_r into the backup element is given in a straightforward way by the second integral (Grace 1993). Rod erosion $v - u$ and target erosion u (penetration rate) in terms of rod length as the independent variable are given respectively as

$$v - u = \left(v_s - u_o\right)\left[1 + \frac{2S_p}{\rho_p\left(v_s - u_o\right)^2} \ln\left(\frac{\ell}{\ell_o}\right)\right]^{1/2}, \tag{2}$$

and

$$u = u_o\left[1 + \frac{2\,S_t}{\rho_t u_o^2} \ln\left(\frac{\ell}{\ell_o}\right)\right]^{1/2}, \tag{3}$$

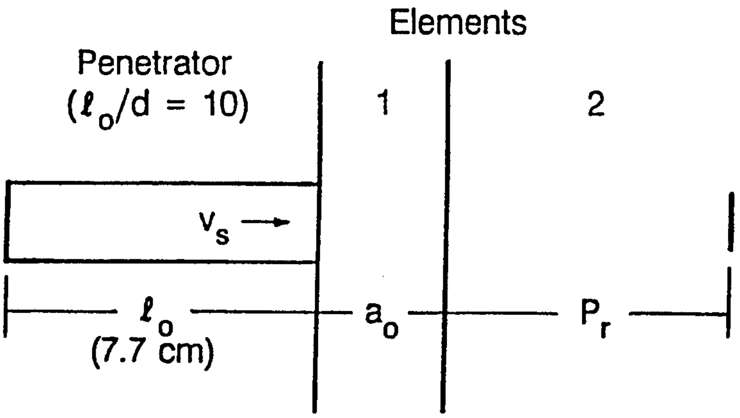

Figure 5. Geometry of Bi-Element-Type Targets.

where u_o is the initial penetration rate; ρ_p and ρ_t are the penetrator and target densities, respectively; and S_p and S_t are the effective penetrator and target strengths, respectively.

When solving equation (1), penetration into the first element is calculated stepwise using small increments of rod length as if the element were semi-infinite. The process continues up to the point where the penetration depth reaches a_o. At that point, the final values from the first integral (v_2, u_2, and ℓ_1) are used to start the penetration process in the second layer. Since equations (3) and (4), as written, apply to the first element, their use for the second element requires v_s, u_o, and ℓ_o to be replaced with v_1, u_1, and ℓ_1. Further, appropriate strengths and densities for the corresponding elements must be included. To check on the validity of dividing the penetration integral into two parts as shown in equation (1), calculations were made for semi-infinite penetration into RHA/RHA- and Ti/Ti-layered targets throughout the entire range of first-layer thickness, and expected results were obtained. Further, accurate penetration depths were obtained for single, semi-infinite targets of both RHA and Ti alloy.

When using equation (1) for bi-element targets of different materials, Grace and Rupert (1993) found that the penetration process through the first-layer can be altered substantially from initial penetration in a semi-infinite target version of the first layer material. The changes are generated by

(1) overall effects of the proximate interface between target layers of different densities, and (2) effects of the time-dependent damage mechanism giving rise to a strength loss if the first layer is a ceramic material. These effects were implemented in the first integral of equation (1) together with equations (2) and (3) through changes in the strength term (S_t) for the target (which was modified to account for time-dependent damage), and changes in the initial penetration rate u_0 (which was adjusted to account for the transient and interface reflection).

3.2 Influence of the Proximate Target/Target Interface. Penetration into the first element was calculated using previous methods (Grace and Rupert 1993) that account for the shock transient, due to impact at the target front surface and shock wave reflections, due to density and sound velocity changes across the target bi-element interface. Treating the first element as semi-infinite produces a penetration process that ignores possible influences, due to the properties of the backup material. This model uses a simplified version of one-dimensional shock wave propagation to treat the influence on penetration due to shock reflection from a proximate interface. An upper limit for the penetration rate is taken to be the particle velocity u_s associated with a shock wave that is generated by penetrator impact with element 1. Two well-known relations [equations (4) and (5)] from the theory of shock wave propagation are as follows:

$$p = \rho u U, \tag{4}$$

and

$$U = c + gu. \tag{5}$$

In these equations, p is the pressure, U is the shock velocity, and u is the particle velocity immediately behind the shock wave. Material properties are given by ρ as density, c as velocity of sound, and g as a material constant. Applying these two equations to the penetrator/target and bi-element target interfaces together with appropriate boundary conditions gives the following expressions used in the current model as

$$u_s = \frac{\rho_p/\rho_1}{1 + \rho_p/\rho_1} v_s, \tag{6}$$

and

$$u_r = (\rho_1/\rho_s)\,u_i, \tag{7}$$

where ρ_p is the rod density, u_r is the velocity of material reflected from the interface, and u_i is the incident material velocity. In equations (4) and (5), under simplifications, the sound speeds of the penetrator and targets are taken to be equal, and the variation of shock speed with particle velocity has been ignored. Upon impact, the initial penetration rate at the front surface u_s drops to a quasi-steady value u_o as penetration proceeds to a depth on the order of a penetrator diameter. The model permits the penetration rate to be increased or reduced from u_o. The change has the form

$$u_e = u_o + q\,(u_s - u_o), \tag{8}$$

where $q\,(u_s - u_o)$ represents an increment of velocity change, and u_o is the initial penetration rate given by previous theory [Grace 1993, equation (25)]. The form of q is arbitrary and chosen to include influences generated by the transient, and the target/target interface is

$$q = \pm k \left(\frac{\rho_2}{\rho_1}\right) \left(\frac{P_1 + d - a_o}{P_1}\right)^2, \tag{9}$$

where d is rod diameter, and P_1 is the DOP into a semi-infinite version of the first-element material. The last term on the right-hand side of equation (9) allows the correction to decrease as the reflective wave weakens, due to increased distance to the reflective boundary as a result of increased applique thicknesses. The ratio of densities across the interface that appears in equation (9) determines the magnitude of the reflected wave, and the sign change indicates the order of densities (positive when $\rho_2 > \rho_1$) (Grace and Rupert 1993; Rupert and Grace 1994). The value for k is chosen so that q can not exceed $q = 1$, and the penetration rate of equation (8) can not exceed u_s. Equations (1), (2), (3), (8), and (9) give the penetration through the first element and the expected rod length and velocity to be used as starting values in the calculation for DOP as given by the second integral of equation (1).

3.3 Time-Dependent Damage Model for Ceramic Strength Loss. Under impact, the ceramic material is subjected to compressive stress at the penetrator/target interface. From this interface, compressive waves travel through the material and reflect from the backing material as compressive or tensile waves. Curran et al. (1993) and Cortés et al. (1992) indicate that the strength of the intact ceramic τ_i increases linearly with hydrostatic stress according to

$$\tau_i = \tau_o + b\sigma, \tag{10}$$

where τ_o is an ambient strength, and b is a strengthening coefficient. The strength of fully damaged or comminuted material τ_c arises from friction only and increases with hydrostatic stress σ as

$$\tau_c = \mu\sigma. \tag{11}$$

The strength of the ceramic in a partially damaged state is derived from these two limiting states through a damage function. Cortés et al. (1992) explored the use of the following damage function [equation (12)] to determine the intermediate strength τ. In their work, the function was interpreted as a mass fraction η of comminuted material within a given volume of material. This function was

$$\tau = (1 - \eta)\,\tau_i + \eta\tau_c. \tag{12}$$

Damage evolution is defined as the rate at which the fraction η evolves toward complete damage. The motivation for evolution develops from the applied hydrostatic stress, σ, above some initial level, σ_o, required for the onset of fracture. The evolution is given by

$$\dot{\eta} = \dot{\eta}_o\,(\sigma - \sigma_o), \tag{13}$$

where $\dot{\eta}_o$ and $\dot{\eta}$ are initial and subsequent time rates of change in the damage fraction as given by Cortés et al. (1992). Although damage evolution is a time-dependent phenomena, time was not explicitly included in their formula since the hydrocode used in their work provided a conditionally determined stress-time history for each material cell during penetration. However, time dependence is included in this report through an explicit $\sigma = \sigma(t)$ function.

The geometric description of the damage model developed by Grace and Rupert (1993) is given in Figure 6 wherein two process zones are defined. Impact of the penetrator with the target front surface produces several wave fronts to be propagated into the material. The first process zone (a) is a manifestation of a subsequent shear wave that defines a region of crazing. Pabst, Steeb, and Claussen (1978) define this process zone as a region of crack nucleation and subcritical, discontinuous crack extension. The maximum propagation rate w_0 of the crack front boundary is assumed to be equivalent to the maximum individual crack velocity, which is related to the Rayleigh wave velocity. However, damage may be initiated by the longitudinal wave within the ceramic. The second process zone (b) is associated with the very highly pressurized region of flow stagnation at the penetrator-target interface. This comminuted zone of fine ceramic particles appears in front of the penetrator, and its influence on penetration has been investigated by Wilkins (1978). In general, the comminuted material has less strength than the intact material. The thickness of this high-pressure zone is taken to remain constant during penetration and to be on the order of a penetrator diameter d. Thus, the high-pressure region (front and rear) travels at the penetration rate u. Both process zone fronts initiate simultaneously at the target front surface upon contact by the penetrator. Thus, the time lapses for each zone to pass a given point P within the ceramic and lying along the penetration centerline are

$$t_a = \left(\frac{P - d}{u} - \frac{P}{w_o} \right), \tag{14}$$

and

$$t_b = \frac{d}{u}, \tag{15}$$

where the subscripts refer to process zones (a) and (b), respectively, and d is the diameter of the penetrator. It is assumed that the damage evolution applies separately to each zone so that

$$\dot{\eta}_a = \dot{n}_{oa} \left(\sigma_a - \sigma_o \right), \tag{16}$$

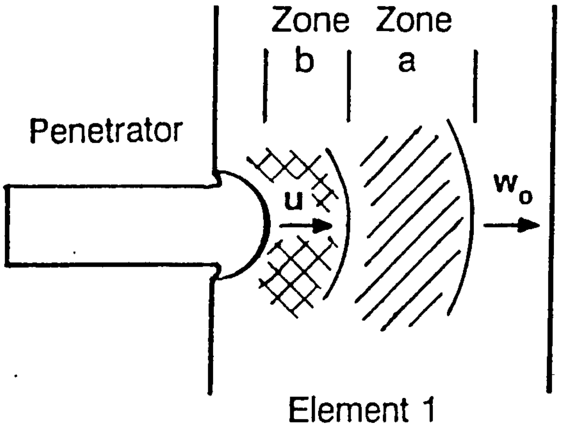

Figure 6. Illustration of the Initial Two Process Zones for the Ceramic Damage Model.

and

$$\dot{\eta}_b = \dot{n}_{ob}\, \sigma_b(t), \tag{17}$$

where σ_a is the overstress taken as constant throughout zone a and $\sigma(t)$ is the stress history of zone (b). For simplicity, it is assumed that the stress distribution in zone (b) is linear with distance within the zone and is also therefore linear with time. The stagnation stress (pressure) σ_s is estimated from application of Bernoulli's equation at a stagnation point on the nose of the penetrator due to target flow. Thus,

$$\sigma_b(t) = \sigma_s \left(\frac{t}{t_b} \right), \tag{18}$$

and

$$\sigma_s = \frac{1}{2} \rho_t\, u^2. \tag{19}$$

Equations (16) and (17) are integrated over the appropriate time intervals to get the damage fractions η_a and η_b. The total damage η at a particular point P is the sum of the cumulative damage in both zones so that

$$\eta = \dot{n}_{oa} \left(\sigma_a - \sigma_o \right) \left(\frac{P - d}{u} - \frac{P}{w_o} \right) + \frac{1}{4} \dot{n}_{ob}\, d\, \rho_t\, u. \tag{20}$$

The damage function equation (20) combines with equation (12) to describe the nominal strength and the extent of ceramic material damage in the present model. For the ceramics, the nominal strength used in the model correlates with the ceramic's dynamic shear strength. This differs from metals, where the model's nominal strength correlates with the metal's dynamic compressive strength. This difference between metals and ceramics in the model's nominal strength selection may relate to the metals tendency to fail due to void nucleation and coalescence vs. the ceramic tendency to fail by means of shear localization. As such, the maximum and minimum shear strengths possible for the ceramic based on the Griffith (1924) brittle fracture criterion are

$$\tau_o = \sigma_{ult}/\sqrt{3}, \tag{21}$$

where σ_{ult} is either the ultimate compressive strength (maximum) or ultimate tensile strength (minimum). For ceramic material undergoing damage, equations (12) and (21) define S_t in equation (3) as the effective stress in the penetration analysis. The damage fraction is computed and S_t is adjusted continually during the numerical integration of the first integral in equation (1).

The analysis describes our efforts through 1993 (Grace and Rupert 1993). We now introduce a third process zone (c) to include the effect of wave reflection at the ceramic/metal interface. The existence of reflected waves and potential subsequent initiation of damage within ceramic targets has been experimentally observed by Hauver et al. (1993). The geometric description of the third process zone is given in Figure 7. At impact, a pressure wave is generated within the ceramic by the penetrator. Once this wave has passed through the ceramic, a reflection from the ceramic/metal interface may initiate the third process zone. The time lapse for third process zone to pass a given point P is

$$t_c = \frac{P - d}{u} - \left(\frac{a_o}{c_o} + \frac{a_o - P}{w_o} \right), \tag{22}$$

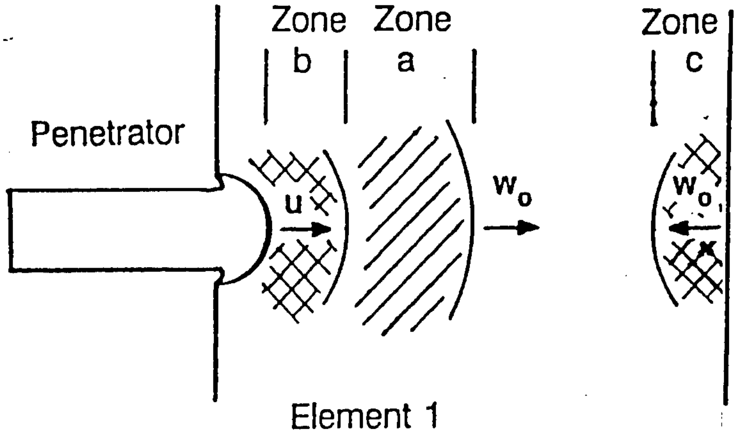

Figure 7. Illustration of the Addition of Third Process Zone for the Ceramic Damage Model.

where the subscript refers to the process zone (c). The damage evolution of process zone (c) is taken to be separate, but can contribute to the overall cumulative damage. Thus,

$$\dot{\eta}_c = \dot{n}_{oc} (\sigma_c - \sigma_o), \tag{23}$$

where σ_c is the over stress taken as a constant throughout zone (c). Equation (23) is integrated over the appropriate time interval to get the damage function η_c. The total damage η at a particular point P is the sum of the cumulative damage in all three zones so that equation (20) becomes

$$\eta = \dot{n}_{oa}\left(\sigma_a - \sigma_o\right)\left(\frac{P-d}{u} - \frac{P}{w_o}\right) + \frac{1}{4}\dot{n}_{ob} d \rho_t u + \dot{n}_{oc}\left(\sigma_c - \sigma_o\right)\left[\frac{P-d}{u} - \left(\frac{a_o}{c_o} + \frac{a_o - P}{w_o}\right)\right]. \tag{24}$$

The damage function equation (24) combines with equation (12) to describe the shear strength and the extent of ceramic material damage in the present model when a third process zone is present.

4. The Size Effect and Weibull Distribution

The Weibull distribution was used to model strength variations within the ceramic applique. The Weibull statistical analysis is based on the weakest link theory (Weibull 1939, 1951), which states that failure is initiated by the lowest required stress at the most critical flaw. This phenomenon yields a size dependance of stress or size effect (McClintock and Argon 1966). In this theory, the probability of failure F can be related to the strength of a specimen through the two-parameter Weibull equation (Weibull 1951; Shih 1980)

$$F = 1 - e^{\int \left(\frac{\sigma}{\sigma_o}\right)^m dV}, \tag{25}$$

where m is the Weibull modulus, σ_0 is a characteristic strength of a unit-volume specimen tested in uniform tension, and σ is the applied stress.

The effective volume KV, or volume of material being tested effectively, is used to predict the strength distribution of one type or size of specimen from that of another. The effective volume is a function of the Weibull modulus and the geometric parameters of the specimen being studied. The effective volume expression can be described analytically for any specimen configuration that possesses a stress distribution that can also be described analytically. The effective volume can be derived for any configuration from the equation

$$KV = \int \left(\frac{\sigma}{\sigma_{max}}\right)^{\frac{1}{m}} dV, \tag{26}$$

where σ is an appropriate expression for the stress distribution, and σ_{max} is the maximum stress. In the case where the stress distribution cannot be described analytically, the effective volume can be computed numerically. Once the effective volume has been determined, the following equation can be used to predict strength levels of equal failure probabilities between specimens of the same material with different dimensions or geometries:

$$\frac{\sigma_1}{\sigma_2} = \left(\frac{KV_2}{KV_1}\right)^{\frac{1}{m}}, \tag{27}$$

where KV_1 is the effective volume of the first specimen configuration and KV_2 is the effective volume of the second (Jadaan et al. 1991). Further, transformation of the control volume from one probability of failure to an another is accomplished using

$$\mathrm{KV}' = \mathrm{KV}\,\frac{\ln(1-F')}{\ln(1-F)}, \tag{28}$$

where KV′ is the new control volume at F′ probability of failure (Johnson and Tucker 1989).

For a first-order approximation of the variation in strength within the ceramic applique, a simplifying assumption was made in regard to the application of the Weibull distribution. It was assumed that the dynamic strength variations within the applique were proportional to strength variations within the three-point bending specimens of the same length and width. This allowed the strength variations to be estimated by combining equations (27) and (28) without solving for the control volume associated with the penetrator target interaction. This resulted in

$$S_t' = \left(\frac{t_w \ln(1-F')}{a_o \ln(1-F)}\right)^{\frac{1}{m}} S_t, \tag{29}$$

where S_t is the dynamic strength, a_o is the applique thickness, and t_w is the three-point bending specimen's thickness used in determining the Weibull modulus. Thus, strength levels S_t at given failure probabilities can be calculated for use in the penetration integral of equation (1).

5. Calculated Results

In this section, the previously developed models for the density effect and material damage are applied to the bi-element targets to first include the ceramic/metal model of Grace and Rupert (1993); second, the adaption of the Weibull distribution to describe the ceramic size effect; and third, the addition of the third process zone to complete the description of the upper and lower performance boundaries. In all cases, striking velocity v_s was 1,500 m/s. Basic material properties used in the initial model calculations are presented in Table 1.

Figure 1 provides a series of model calculations for the alumina/RHA bi-element target. For this target, a series of sequential calculations was conducted. First, to represent penetration into an idealized intact ceramic (undamaged), the nonsteady penetration theory as formulated previously

Table 1. Material Properties Used in the Calculations

Property	DU Alloy	RHA	Alumina
Density (g/cm^3)	18.6	7.85	3.90
Nominal Strength (GPa)	1.38	1.06	2.00
Sound Velocity (m/s)	NU	5,876	10,700

NOTE: NU - not used.

(Grace 1993) was applied with no modification. S_t used in equation (3) was taken as the ceramic's nominal strength of 2.0 GPa from Cortés et al. (1993), which falls within the range discussed by Woodward (1989). The results are analogous to the rule of mixtures as presented in Rupert and Grace (1993). The second curve represents the addition of the density effect where k was set at 0.4. This curve is the expected upper performance bound for the alumina when backed by RHA. The region between curves 1 and 2 represent the predicted performance loss due to the density effect. Thus, the model suggests that data points lying on the second curve could be the result of the ceramic being in an intact state during penetration.

In Figure 1, curve 3 includes both the addition of density effect and the damage model to the calculations. For the damage model, the following constants were used: $\dot{n}_{oa} = 5.0 * 10^{-4}$ Pa^{-1} s^{-1} (Cortés et al. 1992), $\dot{n}_{ob} = 5.0 * 10^{-6}$ Pa^{-1} s^{-1}, σ_o = 100 MPa (Cortés et al. 1992), σ_a = 200 MPa, w_o = 6,000 m/s (McClintock and Argon 1966), and b = 0.1 and μ = 0.37 (Curran et al. 1993). Curve 3 represents a predicted lower performance bound for alumina when backed by RHA. The model predicts that DOP data for alumina/RHA would fall between curves 2 and 3. The model with the time-dependent damage functions indicates that the amount of damage increases with ceramic thickness. Thus, ultimately, the penetration process can transition from a mixed solid/granular flow to one of pure granular flow.

Figures 8 and 9 provide the next series of model calculations for the alumina/RHA bi-element target with ceramic "size" effect taken into account. Calculations were made treating the ceramic layer as (1) intact ceramic with the size effect expressing failure strength in terms of a probabilities, and (2) the addition of the "density" effect to (1) in Figure 8. Adding the time-dependent damage

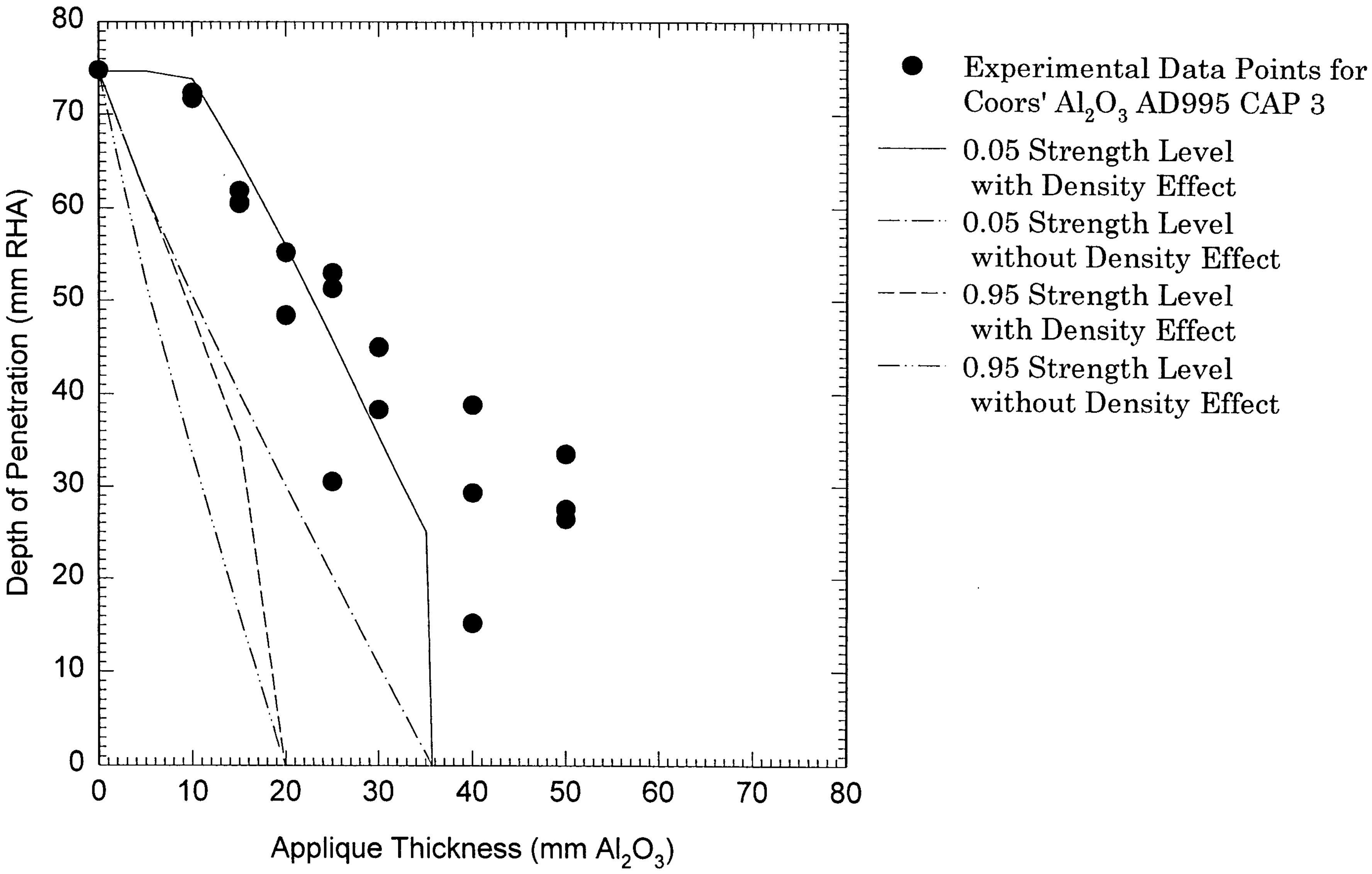

Figure 8. Modeling Results for Intact Al_2O_3/RHA With Ceramic "Size" Effect Added.

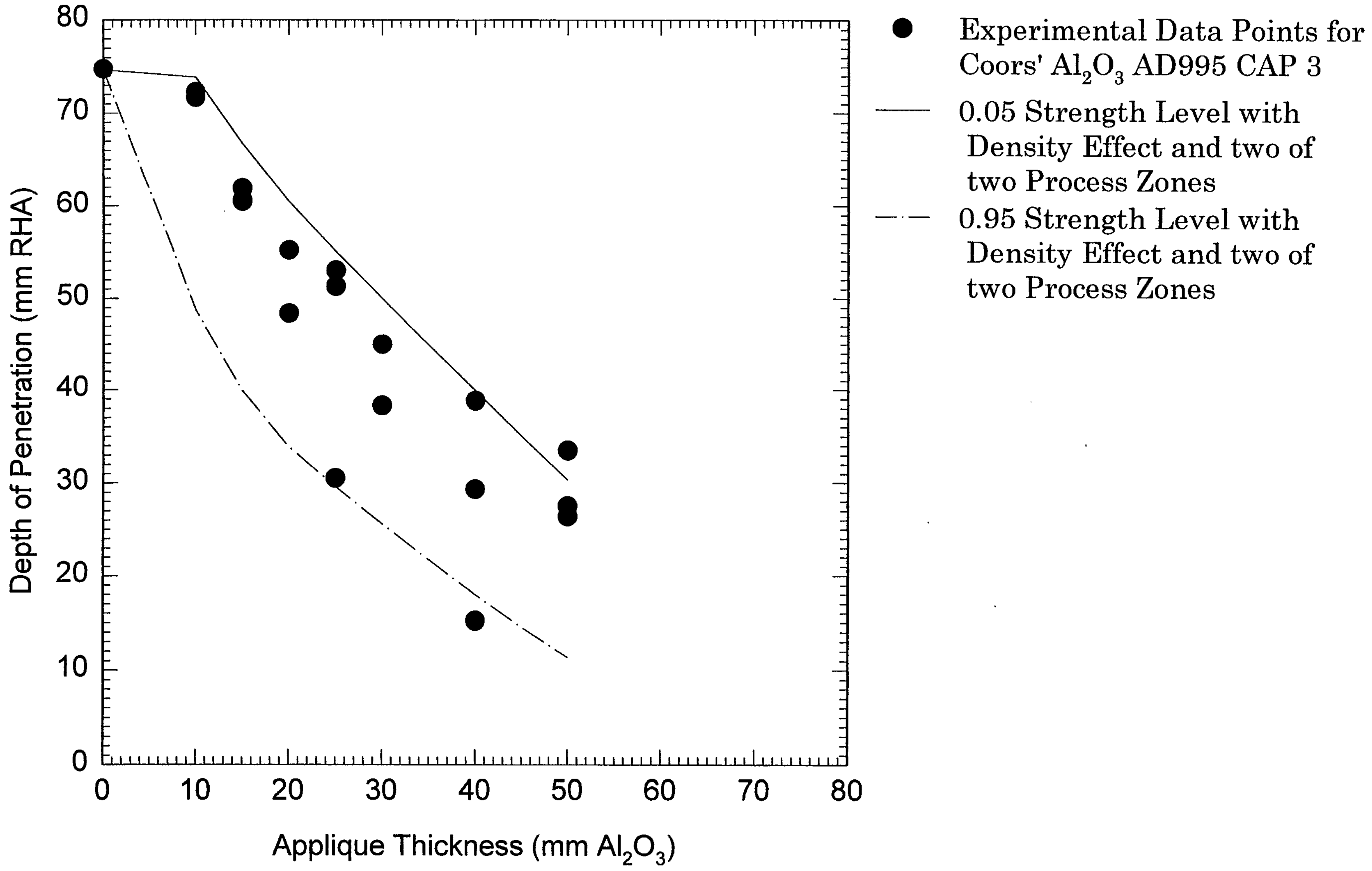

Figure 9. Modeling Results for Al_2O_3/RHA With Ceramic "Size" Effect and Two Process Zones, Time-Dependent Strength Mechanism Added.

mechanisms to (2) is shown in Figure 9. In all cases, striking velocity v_s was 1,500 m/s. The basic model parameters were not changed from the previous set of calculations with the exception of strength. Using equation (29), the ceramic strength (S_t) was set to 2.40 GPa. This corresponds to setting the ceramic strength to $\sigma_{ult}/\sqrt{3}$ for a_o = 25.4 mm (the thickness of the compression sample used to determine the compressive strength) and F' = 0.50. The Weibull parameters used in the model were provided by Paricio (1996) as m = 12.13, t_w = 1.78 mm, and F = 0.50. The probabilities considered were F' = 0.95 and F' = 0.05.

The first set of curves in Figure 8 shows the effect of the probability function for 0.95 and 0.05 intact strength on the predicted penetration. The second set of curves in Figure 8 represents the addition of the density effect on the strength at the two probability levels. Essentially, without the time-dependent mechanism, it would be expected that 90% of the data would be located between the two curves representing the intact ceramic with density effect added. In Figure 9 the time-dependent damage mechanism has been applied to the 0.95 and 0.05 probability levels. The curve at the 0.95 probability with the density effect and time-dependent damage mechanism forms the expected upper density effect as the upper bound as defined in prior work (Grace and Rupert 1993). The curve at the 0.05 is then used to define the lower performance bound for the ceramic response in the DOP tests (upper curve). Further, the analysis suggests that low ceramic performance at large thicknesses cannot be explained by the two process zone model with Weibull distribution and density effects alone. The shape of the lower performance limits indicates a lower value for the coefficient of friction may be required in the model. If the lower coefficient of friction was used in the time-dependent strength model with two process zones to match the data more closely, a greater under prediction of the upper performance bound would occur. Arbitrary adjustments to the strength, coefficient of fraction and damage rates could result in a closer match to either performance boundary, but not both.

Figure 10 address the addition of a possible third process zone into the model's calculations. For these calculations, the coefficient of friction was set at μ = 0.145 (Curran et al. 1993). The damage rate for process zone (a) was equally divided between process zones (a) and (c); $\dot{n}_{oa}$ = 2.5 * 10^{-4} Pa^{-1} s^{-1} and $\dot{n}_{oc}$ = 2.5 * 10^{-4} Pa^{-1} s^{-1}. All other model parameters remained the same as in the

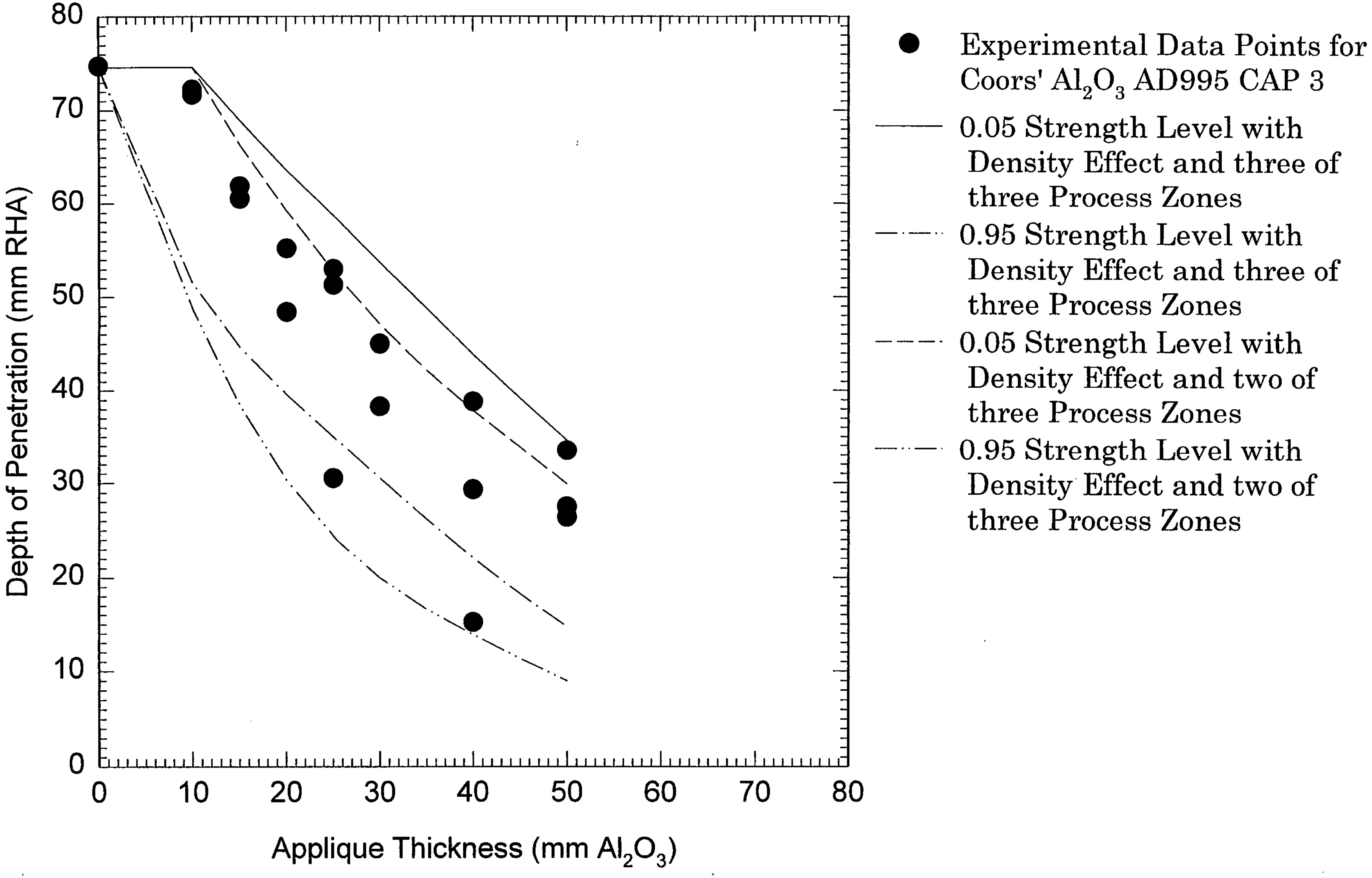

Figure 10. **Modeling Results for Al_2O_3/RHA With Ceramic "Size" Effect and Three Process Zones, Time-Dependent Strength Mechanism Added.**

previous two process zone model. In this version of the model, the upper performance bound was defined as the 0.95 probability curve with only process zones (a) and (b) engaged. This would represent the case of the highest strength and minimum ceramic damage. The lower performance bound was defined as the 0.05 probability curve with all three process zones contributing to the damage of the ceramic. This represents the minimum strength and maximum damage.

6. Conclusions

There are several important conclusions to be drawn from this work.

(1) The evaluation of target materials using DOP testing should take into account the physical phenomena regarding material damage mechanisms and target interaction effects to include the shock-induced transient and wave reflection from target interfaces. Penetration models are needed to account for these effects and to separate the individual contributions. As an example, the current modeling effort explicitly illustrates that the density of the backup element is responsible for a significant target interaction effect, and this can alter ceramic performance substantially.

(2) The modeling of the inherent scatter in ceramic DOP test results has been addressed by accounting for the "size" effect and the intermittent presence of a third process zone. Other factors, such as the scatter introduced by variations in the penetrator (impact velocity, Geometry, strength, etc.) and/or the precision in target fabrication, were not addressed. The ceramic size effect is effectively modeled by adjusting the ceramic's nominal strength using the weakest link theory in terms of the Weibull distribution and measured parameters for the ceramic. The presence of or lack of the third process zone directly effects the scatter observed within the ceramic's performance substantially. As an example, in the current modeling effort, it can be concluded that:

- ceramics modeled with higher Weibull modulus will inheritly predict less scatter in ballistic performance (assuming everything else is equal) as a result of the lower strength variation in the ceramic,

- ceramics targets modeled without an intermittent third process zone will predict less scatter in ballistic performance (assuming everything else is equal),

- ceramics targets modeled without a third process zone will predict a superior upper performance limit compared to ceramic targets modeled with a third process zone (assuming everything else is equal), and

- ceramics targets modeled with a third process zone will predict a degraded lower performance limit compared to ceramic targets modeled without a third process zone (assuming everything else is equal).

(3) Any analysis used in the DOP tests for determining the performance potential of ceramic materials (or any material) under ballistic impact must go beyond recording the residual penetration in the second target element as a function of first element's thickness or areal density for a given impact velocity and penetrator. The analysis needs to be more detailed to determine the actual potential of the ceramic eliminating potential bias introduced through such choices as target geometry and the selection of second target element. With the more indepth analysis, the results from DOP tests become more relevant in predicting actual performance of the ceramic (or any material) in realistic armor systems. The model presented in this report is felt to provide a major step toward accomplishing the link between DOP tests and actual armor performance.

INTENTIONALLY LEFT BLANK

7. References

Cortés, R., C. Navarro, M. A. Martínez, J. Rodríguez, and V. Sánchez-Gálvez. "Numerical Modeling of Normal Impact on Ceramic Composite Armors." *Int. J. Impact Engng.*, vol. 12, pp. 639–651, 1992.

Curran, D. R., L. Seaman, T. Cooper, and D. A. Shockey. "Micromechanical Model for Comminution and Granular Flow of Brittle Material Under High Strain Rate Application to Penetration of Ceramic Targets." *Int. J. Impact Engng.*, vol. 13, pp. 53–83, 1993.

Grace, F. I. "Nonsteady Penetration of Long Rods Into Semi-Infinite Targets." *Int. J. Impact Engng.*, vol. 14, pp. 303–314, 1993.

Grace, F. I., and N. L. Rupert. "Mechanisms for Ceramic/metal, Bi-Element Target." *Proceedings 14th Int. Symp. on Ballistics*, Quebec City, Quebec, Canada, 1993.

Griffith, A. A. "The Theory of Rupture." *Proceedings 1st Int. Con. Appl. Mech. (Delft)*, pp. 55–63, 1924.

Hauver, G. E., P. H. Netherwood, R. F. Benck, and L. J. Kecshes. "Ballistic Performance of Ceramic Targets." *Proceedings of The Army Symposium on Solid Mechanics*, pp. 23–34, Plymouth, MA, 17–19 August 1993.

Jadaan, O. M., D. L. Shelleman, J. C. Conway, Jr., J. J. Mecholsky, Jr., and R. E. Tressler. "Prediction of Strength of Ceramic Tubular Components: Part I - Analysis." *J. Testing and Evaluation*, vol. 19, no. 3, pp. 181–191, 1991.

Johnson, C. A., and W. T. Tucker. "Advanced Statistical Concepts of Fracture in Brittle Materials." *Ceramics Technical Newsletter*, no. 21, 1989.

McClintock, F. A., and A. S. Argon. *Mechanical Behavior of Materials*, Addison-Wesley Publishing Company, Inc., Reading, MA, 1966.

Pabst, R. F., J. Steeb, and N. Claussen. "Microcracking in a Process Zone and its Relation to Continuum Fracture Mechanics." *Fracture Mechanics of Ceramics, Vol 4: Crack Growth and Microstructure*, R. C. Bradt, D. P. H. Hasselman, and F. F. Lange (eds.), Plenum Press, NY, 1978.

Paricio, R. Private communication. Coors Ceramic Company, Structural Product Group, Golden Colorado, 1996.

Rupert, N. L., and F. I. Grace. "Penetration of Long Rods into Semi-Infinite, Bi-Element Targets." *Proceedings 14th Int. Symp. on Ballistics*, Quebec City, Quebec, Canada, 1993.

Rupert, N. L., and F. I. Grace. "Analysis of Defeat Mechanisms for Ceramic/Metal, Bi-Element Targets." Army Science Conference, 1994.

Rupert, N. L., and F. I Grace. "Penetration of Semi-Infinite, Bi-Element Targets by Long Rod Penetrators." ARL-TR-666, U.S. Army Research Laboratory, Aberdeen Proving Ground, MD, January 1995.

Rupert, N. L., and F. I. Grace. "Analysis of Ceramic Defeat Mechanisms: Modeling Variations in Ballistic Data." *Proceedings 20th Army Science Conference*, vol. II, pp. 899–903, June 1996.

Shih, T. T. "An Evaluation of the Probabilistic Approach to Brittle Design." Engineering Fracture Mechanics, vol. 13, pp. 257–271, 1980.

Weibull, W. "A Statistical Theory of the Strength of Materials." *Proceedings of the Royal Swedish Institute of Engineering Research*, no. 151, pp. 1–45, 1939.

Weibull, W. "A Statistical Distribution Function of Wide Applicability." *Jour. Appl. Mech.*, vol. 18, pp. 293–297, 1951.

Wilkins, M. L. "Mechanics of Penetration and Perforation." *Int. J. Engng. Sci.*, vol. 16, pp. 793–807, 1978.

Woodward, R. L. "A Basis for Modeling Ceramic Composite Armor Defeat." MRL-RR-3-89, DSTO Materials Research Laboratory, Melbourne, Victoria, Australia, 1989.

Woolsey, P., S. Mariano, and D. Kokidko. "Alternative Test Methodology for Ballistic Performance Ranking of Armors." *Proceedings 5th TACOM Armor Conference*, March 1989.

NO. OF COPIES	ORGANIZATION
2	DEFENSE TECHNICAL INFORMATION CENTER DTIC DDA 8725 JOHN J KINGMAN RD STE 0944 FT BELVOIR VA 22060-6218
1	HQDA DAMO FDQ DENNIS SCHMIDT 400 ARMY PENTAGON WASHINGTON DC 20310-0460
1	DPTY ASSIST SCY FOR R&T SARD TT F MILTON RM 3EA79 THE PENTAGON WASHINGTON DC 20310-0103
1	OSD OUSD(A&T)/ODDDR&E(R) J LUPO THE PENTAGON WASHINGTON DC 20301-7100
1	CECOM SP & TRRSTRL COMMCTN DIV AMSEL RD ST MC M H SOICHER FT MONMOUTH NJ 07703-5203
1	PRIN DPTY FOR TCHNLGY HQ US ARMY MATCOM AMCDCG T M FISETTE 5001 EISENHOWER AVE ALEXANDRIA VA 22333-0001
1	DPTY CG FOR RDE HQ US ARMY MATCOM AMCRD BG BEAUCHAMP 5001 EISENHOWER AVE ALEXANDRIA VA 22333-0001
1	INST FOR ADVNCD TCHNLGY THE UNIV OF TEXAS AT AUSTIN PO BOX 202797 AUSTIN TX 78720-2797
1	GPS JOINT PROG OFC DIR COL J CLAY 2435 VELA WAY STE 1613 LOS ANGELES AFB CA 90245-5500
1	ELECTRONIC SYS DIV DIR CECOM RDEC J NIEMELA FT MONMOUTH NJ 07703
3	DARPA L STOTTS J PENNELLA B KASPAR 3701 N FAIRFAX DR ARLINGTON VA 22203-1714
1	US MILITARY ACADEMY MATH SCI CTR OF EXCELLENCE DEPT OF MATHEMATICAL SCI MDN A MAJ DON ENGEN THAYER HALL WEST POINT NY 10996-1786
1	DIRECTOR US ARMY RESEARCH LAB AMSRL CS AL TP 2800 POWDER MILL RD ADELPHI MD 20783-1145
1	DIRECTOR US ARMY RESEARCH LAB AMSRL CS AL TA 2800 POWDER MILL RD ADELPHI MD 20783-1145
3	DIRECTOR US ARMY RESEARCH LAB AMSRL CI LL 2800 POWDER MILL RD ADELPHI MD 20783-1145
	ABERDEEN PROVING GROUND
4	DIR USARL AMSRL CI LP (305)

NO. OF COPIES	ORGANIZATION
1	DFNS NUCLEAR AGNCY TECH LIBRARY 6801 TELEGRAPH RD ALEXANDRIA VA 22192
2	HQ DA SARD TR R CHAIT SARD TT J APPEL PENTAGON WASHINGTON DC 20310-0103
3	DIR DARPA R KOCHER (3 CPS) 3701 N FAIRFAX DR ARLINGTON VA 22203-1714
1	PM SURVIVABILITY SYS SFAE ASM SS T T DEAN WARREN MI 48397-5000
1	PM TMAS SSAE AR TMA MT PICATINNY ARSENAL NJ 07806-5000
1	CDR EUROPEAN RSCH OFC USARDSG (UK) R REICHENBACH PSC 802 BOX 15 FPO AE 09499-1500
2	CDR MRDEC AMSMI RD ST WF D LOVELACE M SCHEXNAYER REDSTONE ARSENAL AL 34898-5250
2	CDR NGIC J CRIDER W MARLEY 220 SEVENTH AVE CHARLOTTESVILLE VA 22901-5391
7	CDR TACOM AMCPM ABMS SA J ROWE AMSTA AR TR T FURMANIAK S GOODMAN D HANSEN M MINNICK D THOMAS J THOMPSON WARREN MI 48397-5000
3	CDR ARDEC AMSTA AR AE W J PEARSON TECH LIB AMSTA AR AET M M HESPOS PICATINNY ARSENAL NJ 07806-5000
2	DIR ARO J BAILEY K IYER PO BOX 12211 RESEARCH TRIANGLE PARK NC 27709-2211
1	CHF OF NAVAL RSCH OFC OF NAVAL TECH A J FAULSDITCH ONT 23 BALLSTON TWRS ARLINGTON VA 22217
1	OFC OF NAVAL RSCH CODE 332 J KELLY 800 NO QUINCEY ST ARLINGTON VA 2217-5000
1	NAVAL POST GRAD SCHL CODE EW J STERNBERG MONTEREY CA 93943
2	NAVAL RSCH LAB CODE 6684 A E WILLIAMS CODE 6380 R BADALIANCE 4555 OVERLOOK AVE SW WASHINGTON DC 20375-5343

NO. OF COPIES	ORGANIZATION
2	CDR NSWC J FOLTZ R 32 TECH LIBRARY CARDEROCK DIV BETHESDA MD 20084-5000
5	CDR NSWC DAHLGREN DIV D DICKINSON E ROWE JR B SMITH V GEHMAN TECH LBRY DAHLGREN VA 22448
2	CDR NSWC IH DIV R GARRETT TECH LBRY INDIAN HEAD MD 20640-5035
1	NUSC NEWPORT CODE 8214 S DICKENSON NEWPORT RI 02841
1	CDR NWC TECH LIBRARY CHINA LAKE CA 93555
4	AFAL AFATL DLJW W COOK J FOSTER TECH LBRY W DRESS EGLIN AFB FL 32542
2	AFAL WL MLBM S L DONALDSON MLLN A KATZ WRIGHT PATTERSON AFB OH 45433-7750
2	AMERICAN EMBASSY BONN COL BALD R ROBINSON UNIT 21701 BOX 165 APO AE 09080
1	CIA OSWR DSD W WALTMAN ROOM 5P0110 NHB WASHINGTON DC 20505
1	JET PROPULSION LAB IMPACT PHYSICS GRP M ADAMS 4800 OAK GROVE DR PASADENA CA 91109-8099
15	DIR LANL F ADDESSIO D MANDELL C WINGATE L SCHWALBE M BURKETT E J CHAPYAK MS F664 J V REPA MS A133 M O SCHNICK MS F607 G E CORT F R KAROPA M F GAC B HOGAN W GASKILL S MARSH MS 970 TECH LIB PO BOX 1663 LOS ALAMOS NM 87545
11	DIR LLNL R GOGOLEWSKI MS L290 C CLINE R LANDINGHAM L369 J REAUGH L32 D STEINBERG J E REAUGH L290 M FINGOR MS 35 D BAUM M WILKINS M H MURPHY TECH LIB PO BOX 808 LIVERMORE CA 94550
4	POULTER LAB SRI INTERNATIONAL D CURRAN R KLOOP L SEAMAN D SHOCKEY 333 RAVENSWOOD AVE MENLO PARK CA 94025

NO. OF
COPIES ORGANIZATION

10 DIR SNL
J ASAY MS 0458
D GRADY
E HERTEL JR
R BRANNON MS 0820
L CHABILDAS MS 0821
D CRAWFORD ORG 0821
M FORRESTAL DIV 1551
R GRAHAM DIV
P YARRINGTON
TECH LIB
PO BOX 5800
ALBUQUERQUE NM 87185-0307

2 BROWN UNIV
DIV OF ENGINEERING
R CLIFTON
S SUNDARAM
PROVIDENCE RI 02912

1 ENRGTC MATLS RSCH CTR
NM INST OF MINING & TECH
D EMARY
CAMPUS STATION
SOCORRO NM 87801

1 GA INST OF TECH
K LOGAN
ATLANTA GA 30332-0245

6 IAT
UNIV OF TX AT AUSTIN
S BLESS
H FAIR
T KIEHNE
D LITTLEFIELD
M NORMANDIA
R SUBRAMANIAN
PO BOX 202797
AUSTIN TX 78720-2797

NO. OF
COPIES ORGANIZATION

7 PA STATE UNIV
COLLEGE OF ENGRNG
T KRAUTHAMMER
J CONWAY
R QUEENEY
N SALAMON
R ENGEL
M AMATEAU
A PYTEL
UNIVERSITY PARK PA 16802

3 SW RSCH INST
C ANDERSON
J RIEGEL
J WALKER
PO DRAWER 28510
SAN ANTONIO TX 78284

2 UNIV OF CA SAN DIEGO
DEPT OF APPL MECH
AND ENGR SVCS R011
S NEMAT NASSER
M MEYERS
LA JOLLA CA 92093-0411

4 UNIV OF DAYTON RSCH INST
KLA14
N BRAR
D GROVE
R HOFFMAN
A PIEKUTOWSKI
300 COLLEGE PARK
DAYTON OH 45469-0182

5 UNIV OF TX AT EL PASO
DEPT OF MTLRGCL AND
MATLS ENGRNG
L MURR
EL PASO TX 79968

2 ADELMAN ASSOCIATES
C CLINE
M WILKENS
3301 EL AMINO RIAL STE 280
ATHERTA CA 94027

NO. OF
COPIES ORGANIZATION

1 AEROJET PRECISION WPNS
DEPT 5131 T W
J CARLEONE
1100 HOLLYVALE
AZUSA CA 91702

4 ALLIANT TECHSYSTEMS INC
T HOLMQUIST
C LOPATIN
G JOHNSON
C CANDLAND
23100 SUGARBUSH N
ELK RIVER MN 55343

2 ALLIED SIGNAL
L LIN
PO BOX 31
PETERSBURG VA 23804

3 APLD RSCH ASSOC INC
J D YATTEAU
R RECHT
G RECHT
5941 S MDLFLD RD STE 100
LITTLETON CO 80123

1 APLD RSCH ASSOC INC
D GRADY
4300 SAN MATEO BLVD NE
STE A 220
ALBUQUERQUE NM 87110

2 BATTELLE EDGEWOOD
A RICCHIAZZI
L HERR
2012 TOLLGATE RD STE 206
BEL AIR MD 21014

1 BOEING CORP
T M MURRAY MS 84 84
PO BOX 3999
SEATTLE WA 98124

1 BRIGS CO
J E BACKOFEN
2668 PETERSBOROUGH ST
HERNDON VA 22071-2443

NO. OF
COPIES ORGANIZATION

1 THE CARBORUNDUM CO
R PALIA
PO BOX 1054
NIAGARA FALLS NY 19302

1 CENTURY DYNAMICS INC
N BIRNBAUM
2333 SAN RAMON VLY BLVD
SAN RAMON CA 94583-1613

3 CERCOM INC
A EZIS
G NELSON
R PALICKA
1960 WATSON WAY
VISTA CA 92083

1 COORS CERAMIC CO
STRUCTURAL DIV
600 NINTH ST
GOLDEN CO 80401

1 CORNING INC
S HAGG SP DV 22
CORNING NY 14831

1 CYPRESS INTNL
A CAPONECCHI
1201 E ABINGDON DR
ALEXANDRIA VA 22314

4 DOW CHEMICAL INC
ORDNANCE SYS
K EPSTEIN
C HANEY
A HART
B RAFANIELLO
800 BUILDING
MIDLAND MI 48667

1 DUPONT ADVNC FBRS SYS
B SCOTT
SPRUANCE PLANT
PO BOX 27001
RICHMOND VA 23261

1 E I DUPONT CO
O BERGMANN
BRNDYWN BLDG RM 12204
WILMINGTON DE 19898

NO. OF
COPIES ORGANIZATION

3 DYNA EAST CORP
P C CHOU
R CICCARELLI
W FLIS
3620 HORIZON DR
KING OF PRUSSIA PA 19406

1 EPSTEIN AND ASSOC
K EPSTEIN
2716 WEMBERLY DRIVE
BELMONT CA 94002

5 GDLS
W BURKE
J ERIDON
W HERMAN
P CAMPBELL
D DEBUTCHER
38500 MOUND RD
STERLING HEIGHTS MI
48310-3268

2 GEN RSCH CORP
A CHARTERS
T MENNA
PO BOX 6770
SANTA BARBARA CA
93160-6770

1 INGALLS SHIPBLDG
CBI 01
P GREGORY
PO BOX 149
PASCAGOULA MS 39567

1 INTNL RSCH ASSOC
D ORPHAL
4450 BLACK AVENUE
PLEASANTON CA 94566

1 KAMAN SCIENCES CORP
D BARNETTE
1500 GARDEN OF THE GODS RD
COLORADO SPRINGS CO 80907

NO. OF
COPIES ORGANIZATION

3 LANXIDE ARMR PRDCTS
B FRANZEN
K LEIGHTON
R WOLFE
1300 MARROWS RD
NEWARK DE 19714-6077

1 LIVERMORE SFTWR
TECH CORP
JOHN O HALLQUIST
2876 WAVERLY WAY
LIVERMORE CA 94550

2 LOCKHEED MARTIN
ELCTRCL AND MSL
C E HAMMOND MP 004
L WILLIAMS MP 126
5600 SAND LAKE RD
ORLANDO FL 32819

1 MCDONNELL DOUGLAS
HELICOPTER
L R BIRD
MS 543 D216
5000 E MCDOWELL RD
MESA AZ 85205

4 O'GARA HESS & EISENHARDT
G ALLEN
D MALONE
T RUSSEL
C WILLIAMS
9113 LE SAINT DR
FAIRFIELD OH 45014

2 ORLANDO TECH INC
D MATUSKA
J OSBORN
PO BOX 855
SHALIMAR FL 32579

1 PHYSICS INTL
J COFFENBERRY
2700 MERCED ST
PO BOX 5010
SAN LEANDRO CA 94577

NO. OF COPIES	ORGANIZATION
1	PRIMEX TECH INC R CAMPOLI 200 E HIGH ST PO BOX 127 RED LION PA 17356
1	PRIMEX TECH INC D EDMONDS 10101 9TH ST N ST PETERSBURG FL 33716
1	RAYTHEON CO R LLOYD PO BOX 1201 TEWKSBURY MA 01876
1	ROCKWELL INTL ROCKETDYNE DIV J MOLDENHAUER 6633 CANOGA AVE HB 23 CANOGA PK CA 91303
1	SAIC J FURLONG MS 264 1710 GOODRIDGE DR MCLEAN VA 22102
3	SIMULA INC G GRACE R HUYETT G YANIU 10016 SOUTH 51ST STREET PHOENIX AZ 85044
1	STARMET CORP R QUINN 2229 MAIN ST CONCORD MA 01742
1	TRACOR AEROSPACE INC R BROWN PO BOX 196 SAN RAMON CA 94566

NO. OF COPIES	ORGANIZATION
4	UTD DFNS LP V HORVATICH M MIDDIONE J MORROW R RAJAGOPAL PO BOX 359 SANTA CLARA CA 95052-0359
1	UTD DFNS LP J JOHNSON PO BOX 15512 YORK PA 17405-1512
1	ZERNOW TECH SVCS INC L ZERNOW 425 W BONITA AVE STE 208 SAN DIMAS CA 91773
1	R J EICHELBERGER 409 W CATHERINE ST BEL AIR MD 21014-3613
1	B EINSTEN 1212 MORNINGSIDE WAY VENICE CA 90297
1	B SKAGGS RT 11 BOX 81E SANTA FE NM 87501

NO. OF COPIES	ORGANIZATION
	ABERDEEN PROVING GROUND
116	DIR ARL
	AMSRL WM T, W MORRISON
	AMSRL WM TA,
	S BILYK
	W BRUCHEY
	W GILLICH
	T HAVEL
	E HORWATH
	Y HUANG
	H MEYER
	E J RAPACKI
	N RUPERT (25 CPS)
	W GOOCH JR
	G HAUVER
	J DEHN
	M BURKINS
	AMSRL WM TC,
	A COPLAND
	W S DE ROSSET
	F GRACE (25 CPS)
	K KIMSEY
	M LAMPSON
	W LEONARD
	L MAGNESS
	D SCHEFFLER
	G SILSBY
	R SUMMERS
	W WALTERS
	AMSRL WM TD,
	S CHOU (16 CPS)
	A M DIETRICH
	T FARRAND
	K FRANK
	A GUPTA
	P KINGMAN
	M RAFTENBERG
	M SCHEIDLER
	S SEGLETES
	J WALTER
	T WRIGHT
	AMSRL WM TE, A NIILER
	AMSRL WM M,
	D VIECHNICKI
	J McCAULEY
	AMSRL WM MC,
	M CHEN
	G GILDE
	P HAUNG
	T HYNES
	J SWAB
	J WELLS
	J LASALVIA
	AMSRL WM MF,
	D DANDEKAR
	R RAJENDRAN
	AMSRL WM ME,
	M STAKER
	R ADLER
	AMSRL WM MD,
	W ROY
	R DOWDING
	AMSRL WM MB

NO. OF COPIES	ORGANIZATION
10	AERONAUTICAL & MARITIME RESEARCH LABORATORY N BURMAN G WESTON M CHICK A MOURITZ E GELLERT S PATTIE R J CHESTER J DIMAS S CIMPOERU D PAUL PO BOX 4331 MELBOURNE VIC 3001 AUSTRALIA
1	ATS1 LOGISTICS SYSTEMS AGENCY R WILLIAMS LAVERTON 3027 AUSTRALIA
1	BATTELLE INGENIEURTECHNIK GMBH W FUCKE DUESSELDORFFER STR 9 ESCHBORN D 65760 GERMANY
1	CARLOS III UNIV OF MADRID C NAVARRO ESCUELA POLITÉENICA SUPERIOR C/. BUTARQUE 15 28911 LEGANÉS MADRID SPAIN
1	CELSIUS MATERIALTEKNIK KARLSKOGA AB L HELLNER S 691 80 KARLSKOGA SWEDEN
5	CENTRE D'ETUDES GRAMAT J CAGNOUX C GALLIC M CAURET P CHARTAGNAC J TRANCHET GRAMAT 46500 FRANCE
9	CENTRE DE RECHERCHES ET D'ETUDES D'ARCUEIL D BOUVART C DENOUAL C COTTENNOT S JONNEAUX H ORSINI S SERROR F TARDIVAL D'ETUDES D'ARCUEIL 16 BIS AVENUE PRIEUR DE LA CÔTE D'OR F 94114 ARCUEIL CÉDEX FRANCE
2	CONDAT J KIERMEIR K THOMA MAXILLANSTR 28 8069 SCHEYERN FERNHAG GERMANY
2	DEFENCE TECH & PROCUREMENT AGCY G LAUBE W ODERMATT BALLISTICS WPNS & COMBAT VEH TEST CTR CH 3602 THUN SWITZERLAND
4	DEFENCE RESEARCH AGENCY T BARTON P CHURCH I CULLIS M J HINTON FORT HALSTEAD SEVENOAKS KENT TN14 7BP UNITED KINGDOM

NO. OF
COPIES ORGANIZATION

5 DEFENCE RESEARCH AGENCY
W CARSON
I PICKUP
T HAWKINS
B JAMES
B SHRUBSALL
CHOBHAM LANE
CHERTEY SURREY KT16 OEE
UNITED KINGDOM

1 DEFENCE RSCH ESTAB SUFFIELD
C WEICKERT
BOX 4000 MEDICINE HAT
ALBERTA TIA 8K6
CANADA

1 DEFENCE RESEARCH ESTAB
VALCARTIER (DREV)
WPN SYS DIV
D NANDALL
CP 8800 COURCELETTE
PQ GOA 1RO
CANADA

1 DEFENCE SCIENTIFIC ESTAB
P RIDDELL
AUCKLAND NAVAL BASE
AUCKLAND 9
NEW ZEALAND

1 DEUTSCHE AEROSPACE AG
M HELD
POSTFACH 13 40
D 86 523 SCHROBENHAUSEN
GERMANY

3 DEUTSCHE FRANZÖSISCHES
FORSCHUNGSINSTITUT
SAINT LOUIS
H ERNST
K HOOG
H LERR
CÉDEX 5 RUE DU GÉNÉRAL
CASSAGNOU
F 68301 SAINT LOUIS
FRANCE

NO. OF
COPIES ORGANIZATION

1 DIEHL GMBH AND CO
M SCHILDKNECHT
FISCHBACHSTRASSE 16
D 90552 RÖTBENBACH AD
PEGNITZ
GERMANY

1 DYNAMIC RESEARCH AB
Ä PERSSON
PARADISGRÄND 7
SÖDERTÄLJE S 151 36
SWEDEN

1 ESQUMALT DEFENCE RESEARCH
DETACHMENT
A J RUSSELL
FMO VICTORIA B C
VOS 1BO
CANADA

1 ETBS DSTI
P BARNIER
ROUTE DE GUERAY
BOITE POSTALE 712
18015 BOURGES CEDEX
FRANCE

1 EMBASSY OF AUSTRALIA
R WOODWARD
COUNSELLOR DEFENCE
SCIENCE
1601 MASS AVE NW
WASHINGTON DC 20036-2273

2 FEDERAL MINISTRY OF
DEFENCE
DIR OF EQUIPMENT AND
TECH LAND
RÜV 2
D HAUG
L REPPER
POSTFACH 1328
53003 BONN
GERMANY

NO. OF COPIES	ORGANIZATION
2	FRANHOFER INSTITUT FÜR KURZZEITDYNAMIK ERNST MACH INSTITUT V HOHLER K THOMA ECKERSTRASSE 4 D 79 104 FREIBURG GERMANY
4	FRANHOFER INSTITUT FÜR KURZZEITDYNAMIK ERNST MACH INSTITUT H ROTHENHÄUSLER K WINEMANN H SENF E STRASSBURGER HAUPTSTRASSE 18 D 79 576 WEIL AM RHEIN GERMANY
2	HIGH ENERGY DENSITY RESEARCH CTR V FORTOV G KANEL IZHORSKAYA STR 13/19 MOSCOW 127412 RUSSIAN REPUBLIC
1	INGENIEURBÜRO DEISENROTH F DEISENROTH AUF DE HARDT 33 35 D 5204 LOHMAR 1 GERMANY
1	INST OF CHEMICAL PHYSICS S RAZORENOV 142432 CHERNOGOLOVKA MOSCOW REGION RUSSIAN REPUBLIC
7	INSTITUTE FOR PROBLEMS IN MATERIALS SCIENCE S FIRSTOV B GALANOV O GRIGORIEV V KARTUZOV V KOVTUN Y MILMAN V TREFILOV 3, KRHYZHANOVSKY STR 252142, KIEV-142, UKRAINE
1	INSTI FOR PROBLEMS OF STRESS G STEPANOV TIMIRYAZEVSKAYA STR 2 252014 KIEV UKRAINE
3	INST OF MECHANICAL ENGINEERING PROBLEMS V BULATOV D INDEITSEV Y MESCHERYAKOV BOLSHOY, 61, V.O. ST PETERSBURG, 199178 RUSSIAN REPUBLIC
2	IOFFE PHYSICO TECH INST E DROBYSHEVSKI A KOZHUSHKO ST PETERSBURG 194021 RUSSIAN REPUBLIC
1	K&W THUN W LANZ ALLMENDSSTRASSE 86 CH 3602 THUN SWITZERLAND
2	MONASH UNIVERSITY DEPARTMENT OF CIVIL ENG R GRZEBIETA (2 CPS) CLAYTON VICTORIA 3168 AUSTRALIA

NO. OF COPIES	ORGANIZATION
1	MORGAN MATROC C ROBERTSON ST PETERS RD RUGBY WARWICKSHIRE CV 21 3QR UNITED KINGDOM
10	NATIONAL DEFENCE RSCH ESTAB J ERIKSON S SAVAGE L WESTERLING P LUNDBERG P-O OLSSON L-G OLSSON H OSKARSSON S-O StÅHL K RAGNARSSON K EKELUND FOA 630 S 172 90 STOCKHOLM SWEDEN
1	R OGORKIEWICZ 18 TEMPLE SHEEN LONDON SW 14 7RP UNITED KINGDOM
1	OTO BREDA M GUALCO M PELLEGRI VIA VALDIOCCHI 15 I 19136 LA SPEZIA ITALY
5	RAFAEL BALLISTICS CENTER M MAYSELESS Y PARTOM G ROSENBERG Z ROSENBERG Y YESHURUN PO BOX 2250 HAIFA 31021 ISRAEL
1	RSCH INST OF MECHANICS NIZHNIY NOVGOROD STATE UNIV A SADYRIN PR GAYARINA 23 KORP6 NIZHNIY NOVGOROD 603600 RUSSIAN REPUBLIC
1	ROYAL MILITARY ACADEMY E CELENS RENAISSANCE AVE 30 B 1040 BRUSSELS BELGIUM
1	ROYAL NETHERLANDS ARMY J HOENEVELD V D BURCHLAAN 31 PO BOX 90822 2509 LS THE HAGUE NETHERLANDS
3	SNPE P FABRE C GAUDIN C GOUZOUGUEN BP NO 2 91710 VERT-LE-PETIT FRANCE
3	SWEDISH DEFENCE RSCH ESTAB L HOLMBERG B JANZON I MELLGARD BOX 551 S 147 25 TUMBA SWEDEN
1	TECHNION INST OF TECH FACULTY OF MECH ENGINEERING S BODNER TECHNION CITY HAIFA 32000 ISRAEL
3	TECHNISCHE UNIVERSITÄT CHEMNITZ-ZWICKAU I FABER L KRUEGER L MEYER SCHEFFEL STR 110 09120 CHEMNITZ GERMANY

NO. OF
COPIES ORGANIZATION

3 TNO PRINS MAURITS LAB
H PASMAN
G PESKES
R YSSELSTEIN
PO BOX 45
LANGE KLEIWEG 137
2280 AA RIJSWIJK
NETHERLANDS

2 TOMSK BR OF THE INST
FOR STRUCTURAL
MACROKINETICS
V GORELSKI
S ZELEPUGIN
8 LENIN SQ GSP 18
TOMSK 634050
RUSSIAN REPUBLIC

1 RESEARCH AND DEV. DEPT.
EMPRESA NACIONAL SANTA
BÁRBARA
C BRIALES
CARRETERA DE BELVIS KM 1
PARACUELLOS DEL JARAMA
28860 MADRID
SPAIN

6 DEPARTAMENTO DE CIENCIA
DE MATERIALES
E T S DE INGENIEROS DE
CARMINOS
R CORTÉS
R ZAERA
M A MARTINEZ
V SÁNCHEZ-GÁLVEZ
M VIGIL
I S CHOCRON-BENLOULO
CANALES Y PUERTOS
UNIVERSIDAD POLITÍCNICA DE
MADRID
CIUDAD UNIVERSITARIA
E 28040 MADRID
SPAIN

NO. OF
COPIES ORGANIZATION

4 MILITARY UNIVERSITY OF TECH
2 KALISKIEGO STREET
K JACH
M MROCZKOWSKI
R ŚWIERCZYŃSKI
E WLODARCZYK
01 489 WARSAW 49
POLAND

1 MENDEL UNIVERSITY OF
AGRICULTURE AND FORESTRY
ZEMĚDĚLSKA 1
J BUCHAR
61300 BRNO
CZECH REPUBLIC

1 MILITARY RESEARCH INST
ZÁHORIE
M LAZAR
905 24 SENICA
SLOVAK REPUBLIC

1 MILITARY RESEARCH INST
RYBKOVA 2A
S ROLE
P O B 547
602 00 BRNO
CZECH REPUBLIC

1 NUCLEAR POWER PLANT
RESEARCH INSTITUTE
OKRUŽNÁ 5
V ADAMIK
918 64 TRNAVA
SLOVAK REPUBLIC

1 MASARYK UNIVERSITY
BURESOVA
J HŘEBIČEK
600 00 BRNO
CZECH REPUBLIC

1 DEMEX CONSULTING ENG.
A/S
S MADSEN
HEJREVEJ 26,
DK 2400 KØBENHAUN
DENMARK

NO. OF COPIES	ORGANIZATION
4	CENTURY DYNAMICS LTD DYNAMICS HOUSE N FRANCIS I LIVINGSTONE R CLEGG C HAYHURST HURST ROAD HORSHAM WEST SUSSEX RH12 2DT ENGLAND UNITED KINGDOM
1	CISI SOCIETY AVENUE J F KENNEDY F GILL BP19 33702 MÉRIGNAC CÉDEX FRANCE
4	CRANFIELD UNIVERSITY ROYAL MILITARY COLLEGE OF SCIENCE SHRIVENHAM R LUMLEY P HAZELL M IREMONGER I HORSFALL SWINDON SN6 8LA UNITED KINGDOM
2	DEFENCE RESEARCH ESTAB. VALCARTIER R DELGRAVE D NANDLALL P O BOX 8800 COURCELETTA QUÉBEC GOA IRO CANADA
1	LABORATOIRE DE MÉCANIQUE ET TECHNOLOGIE F HILD ENS DE CACHAN CNRS UNIVERSITÉ PARIS 6 61 AVENUE DU PRÉSIDENT WILSON F 94235 CACHAN CEDEX FRANCE
2	CENTRE DE RECHERCHES ET D'ETUDES D'ARCUEIL 16 BIS AVENUE PRIEUR DE LA CÔTE D'OR F 94114 ARCUEIL CÈDEX FRANCE
1	CELSIUS MATERIAL TEKNIK KARLSKOGA AB S 691 80 KARLSKOGA SWEDEN
1	SWISS FEDERAL ARMAMENT WORKS W LANZ ALLMENDSSTRASSE 86 CH 3602 THUN SWITZERLAND
2	HIGH ENERGY DENSITY RSRCH CENTER G KANEL V FORTOV IZHORSKAYA 13 19 MOSCOW 127412 RUSSIAN REPUBLIC

REPORT DOCUMENTATION PAGE

Form Approved
OMB No. 0704-0188

1. AGENCY USE ONLY ***(Leave blank)***

2. REPORT DATE
May 1998

3. REPORT TYPE AND DATES COVERED
Final, Oct 95 - Jan 97

4. TITLE AND SUBTITLE
Modeling Ceramic Defeat Mechanisms and Variations in Ballistic Data

5. FUNDING NUMBERS
AH80

6. AUTHOR(S)
Nevin L. Rupert and Fred I. Grace

7. PERFORMING ORGANIZATION NAME(S) AND ADDRESS(ES)
U.S. Army Research Laboratory
ATTN: AMSRL-WM-TA
Aberdeen Proving Ground, MD 21005-5069

8. PERFORMING ORGANIZATION REPORT NUMBER
ARL-TR-1670

9. SPONSORING/MONITORING AGENCY NAMES(S) AND ADDRESS(ES)

10.SPONSORING/MONITORING AGENCY REPORT NUMBER

11. SUPPLEMENTARY NOTES

12a. DISTRIBUTION/AVAILABILITY STATEMENT
Approved for public release; distribution is unlimited.

12b. DISTRIBUTION CODE

13. ABSTRACT ***(Maximum 200 words)***

Bi-element or layered targets have been used to obtain depth-of-penetration (DOP) data so that performance of ceramic materials under ballistic impact can be evaluated. While the data have been particularly useful for ranking ceramics as possible armor candidates, interpretation of the data has been difficult and little insight into the dynamics and mechanisms of the penetration process has been obtained from such data. Prior analytical work into the penetration mechanics of ceramics by the authors included two important factors (i.e., a dynamic target interaction resulting from pressure wave reflection at the interface between target elements and a time-dependent damage mechanism describing the response of the ceramic material). In the present work, a "size" effect, known to be associated with ceramic behavior, and the introduction of a third process zone have been included in the analysis to address a portion of the variations (scatter) in the DOP test data. The analysis now includes results of the weakest-link theory in terms of the Weibull distribution and measured parameters for Al_2O_3. Calculated results are compared with the original data and prior analysis to provide relationships between all three mechanisms and indicate the influence of the size effect on the data.

14. SUBJECT TERMS
penetration modeling, Weibull distribution, Rupert-Grace penetration model, Grace-Tate penetration theory, depth-of-penetration tests, ceramics

15. NUMBER OF PAGES
44

16. PRICE CODE

17. SECURITY CLASSIFICATION OF REPORT	**18. SECURITY CLASSIFICATION OF THIS PAGE**	**19. SECURITY CLASSIFICATION OF ABSTRACT**	**20. LIMITATION OF ABSTRACT**
UNCLASSIFIED	UNCLASSIFIED	UNCLASSIFIED	UL

NSN 7540-01-280-5500

Standard Form 298 (Rev. 2-89)
Prescribed by ANSI Std. 239-18 298-102

INTENTIONALLY LEFT BLANK.

USER EVALUATION SHEET/CHANGE OF ADDRESS

This Laboratory undertakes a continuing effort to improve the quality of the reports it publishes. Your comments/answers to the items/questions below will aid us in our efforts.

1. ARL Report Number/Author ARL-TR-1670 (Rupert) __________ Date of Report May 1998

2. Date Report Received __________

3. Does this report satisfy a need? (Comment on purpose, related project, or other area of interest for which the report will be used.) __________

4. Specifically, how is the report being used? (Information source, design data, procedure, source of ideas, etc.) __________

5. Has the information in this report led to any quantitative savings as far as man-hours or dollars saved, operating costs avoided, or efficiencies achieved, etc? If so, please elaborate. __________

6. General Comments. What do you think should be changed to improve future reports? (Indicate changes to organization, technical content, format, etc.) __________

CURRENT ADDRESS

Organization

Name E-mail Name

Street or P.O. Box No.

City, State, Zip Code

7. If indicating a Change of Address or Address Correction, please provide the Current or Correct address above and the Old or Incorrect address below.

OLD ADDRESS

Organization

Name

Street or P.O. Box No.

City, State, Zip Code

(Remove this sheet, fold as indicated, tape closed, and mail.)

(DO NOT STAPLE)